

Concordant estimates of oceanic carbon monoxide source and sink processes in the Pacific yield a balanced global “blue-water” CO budget

Oliver C. Zafiriou

Woods Hole Oceanographic Institution, Woods Hole, Massachusetts, USA

Steven S. Andrews

Department of Zoology, University of Cambridge, Cambridge, UK

Wei Wang

Woods Hole Oceanographic Institution, Woods Hole, Massachusetts, USA

Received 18 September 2001; revised 7 March 2002; accepted 8 March 2002; published 12 February 2003.

[1] Studies to characterize sources and sinks of carbon monoxide (CO) in the mixed layer were carried out at sites covering large regions of the north and south Pacific. Apparent quantum yield spectra for the photochemical production of CO from colored dissolved organic matter were measured, as were first-order net microbial CO consumption rate constants. Contrary to initial expectations, neither photoproduction nor biooxidation parameters exhibited strong regional variations, except that in the Southern Ocean CO biooxidation rate coefficients were very low. Global “blue-water” CO flux terms derived from the data (in Tg carbon from CO per year, CO-C a⁻¹) are: photochemical source, 50 (estimated range, 30–70), microbial sink, 32 (estimated range, 10–60) and total CO sink (microbial plus gas exchange), 38 (estimated range, 13–60). Considering uncertainties and extrapolation biases, these independently estimated source and sink terms are thus in, or close to, balance at ~40 (range of overlap, 30–60) Tg CO-C a⁻¹. The simplest interpretation of this balance is that no major net sources or sinks (i.e., light-independent production, photoproduction at >450 nm) remain undiscovered, though considerable uncertainty in actual process rates remains. These CO fluxes are, however, very much smaller than some recently estimated values. The origins and implications of these discrepancies are discussed, and the coastal budget term is approximated. *INDEX TERMS*: 0330 Atmospheric Composition and Structure: Geochemical cycles; 1615 Global Change: Biogeochemical processes (4805); 1699 Global Change: General or miscellaneous; *KEYWORDS*: oceanic carbon monoxide sources and sinks, microbial oxidation of carbon monoxide in sea water, photochemical production of carbon monoxide in the Pacific, balanced carbon monoxide budget, apparent quantum yield spectrum of carbon monoxide, colored dissolved organic matter and carbon monoxide

Citation: Zafiriou, O. C., S. S. Andrews, and W. Wang, Concordant estimates of oceanic carbon monoxide source and sink processes in the Pacific yield a balanced global “blue-water” CO budget, *Global Biogeochem. Cycles*, 17(1), 1015, doi:10.1029/2001GB001638, 2003.

1. Introduction

[2] Swinnerton *et al.* [1970] noted diurnal changes in sea-surface [CO], a phenomenon that has been found to be broadly observable, usually with large amplitudes [Bullister *et al.*, 1982; Conrad *et al.*, 1982; Jones, 1991; Bates *et al.*, 1995; Johnson and Bates, 1996; Ohta *et al.*, 1999; H. Xie *et al.*, Diurnal cycling of carbon monoxide in Sargasso Sea surface waters, manuscript in preparation 2002 (here-

inafter referred to as Xie *et al.*, manuscript in preparation, 2002)]. Mean ocean [CO] values and biooxidation rate constants from the literature are summarized in Table 1a. The diurnal scale of variability is imposed by the CO source: production by solar photolysis of colored dissolved organic matter (CDOM) [Bullister *et al.*, 1982; Conrad *et al.*, 1982; Redden, 1982; Gammon and Kelly, 1990; Zuo and Jones, 1995]. Large diurnal amplitudes require fast-acting sinks that are provided by microbial oxidation [Conrad and Seiler, 1980, 1982; Conrad *et al.*, 1982; Jones and Morita, 1984a; Jones and Amador, 1993], and gas exchange [Conrad *et al.*, 1982; Conrad and Seiler,

Table 1a. Marine Carbon Monoxide Mixed-Layer Concentrations and Biooxidation Rate Coefficients

Region	Value	Comments	References
<i>CO Concentration, ^anmole/kg</i>			
Atlantic	2.2	1 cruise	<i>Conrad et al.</i> [1982]
Pacific	0.96	60°N–60°S mean, 8 cruises	<i>Bates et al.</i> [1995]
Global average	1.4	area-weighted Atlantic and Pacific means	
<i>Bio-oxidation rate coefficients, ^bday⁻¹</i>			
North Atlantic	0.69 to 0.66	n = 3 (time-series incubations)	<i>Conrad et al.</i> [1982]
North Atlantic	0.06 to 0.89	Sargasso <100 m, n = 12, median = 0.28	<i>Jones</i> [1991]
Eastern Caribbean and North Atlantic	0.22 to 0.96	blue-water, n = 8, median = 0.26	<i>Jones and Amador</i> [1993]
As above, coastal	1.3 to 12	n = 23, median = 3.4	<i>Jones and Amador</i> [1993]

^aAt ~4–5 m, using underway sampling systems. Averages given are of large (>10³ points) data set.

^bExponentially fit CO loss, ¹⁴CO → ¹⁴CO₂ incubations (gross rates) unless otherwise noted. Net rates are from unlabeled incubations. Values reported in this work are found in Table 4 and Figures 5–8.

Table 1b. Marine Carbon Monoxide Mixed-Layer (ML) Flux Estimates^a

Region	Value	Comments	References
<i>CO Photoproduction (Tg CO-C a⁻¹)</i>			
Globally extrapolated N. and S. Atlantic data	>(4.3 to 47) ^b	We assume that photoproduction must equal or exceed gas-exchange.	<i>Conrad et al.</i> [1982]
Globally extrapolated N. and S. Atlantic data	>71 ± 34 ^b	See gas exchange term below.	<i>Erickson</i> [1989]
Globally extrapolated coastal/shelf waters	130–170	Irradiations of 11 fresh natural waters; optical/insolation model.	<i>Valentine and Zepp</i> [1993]
Globally extrapolated N. Atlantic data (Sargasso)	510 ± 90 ^c (~46 coastal)	13 sites, n = 98. Correlation of sample irradiation data with seawater [DOC] (r ² = 0.72), insolation, and global [DOC] estimate.	<i>Zuo and Jones</i> [1995]
Globally extrapolated N. Atlantic (Azores)	>21–342 ^c	We assume that photoproduction must equal or exceed gas-exchange.	<i>Springer-Young et al.</i> [1996]
Globally extrapolated	820	From sample irradiations. Optical and insolation models and apparent quantum yield data of <i>Valentine and Zepp</i> [1993]	<i>Moran and Zepp</i> [1997]
<i>CO Bio-oxidation^d (Tg CO-C a⁻¹)</i>			
Global, >200 m	21 ^d	k _{bio} = 0.27 (median); [CO] _{av} , 1.4; ML depth, 40 m.	
Global coastal	19 ^d	k _{bio} = 3.4 (median); [CO] _{av} , 1.4; ML depth, 40 m.	
Total Global	40 ^d	Sum of coastal and >200 m estimates.	
<i>Sea → Air Exchange (Tg CO-C a⁻¹)</i>			
Globally extrapolated N. and S. Atlantic data	4.3 to 47 ^b	[CO], wind speeds, air-sea gas exchange algorithm. Hourly data, ~50 days.	<i>Conrad et al.</i> [1982]
Globally extrapolated N. and S. Atlantic data	71 ± 34 ^b	Light, [DOM] and wind fields, with air-sea exchange algorithm and a linear [CO]-light relation calibrated with data of <i>Conrad et al.</i> [1982].	<i>Erickson</i> [1989]
Global	16	Basis not stated.	<i>Khalil and Rasmussen</i> [1990]
Globally extrapolated Pacific data	<80	Pacific [CO], wind speeds, Wanninkhof's air-sea gas exchange algorithm.	<i>Gammon and Kelly</i> [1990]
Globally extrapolated Pacific data	5.6 (3 to 11)	~5000 multi-year, six-cruise Pacific [CO] values, COADS winds, gas exchange algorithms.	<i>Bates et al.</i> [1995]

Table 1b. (continued)

Region	Value	Comments	References
Globally extrapolated N. Atlantic data	510 ± 90^c	CO photo-production estimate and their assumption that most CO outgases.	Zuo and Jones [1995]
Globally extrapolated N. Atlantic (Azores)	21–342 ^e	Air-side [CO] profile gradients. Net flux includes surface microlayer terms.	Springer-Young et al. [1996]

^aEstimates of CO source and sink terms from this work are shown in Table 3, Table 4, and in Figure 9.

^bLinked values, we assume the stated CO sea \rightarrow air flux is supplied by CO photo-production.

^cLinked values, we assume that the CO sea-air flux essentially equals their source flux estimate.

^dFrom literature values (Table 1a) plus our area and depth assumptions. Results are products of median k_{bio} , $[CO]_{av}$ (Table 1a), and areas of regions indicated, for a ML depth of 40 m.

^eRange based on $85.7 \pm$ “at least a factor of 2–4” [Springer-Young et al., 1996].

1982; Erickson, 1989; Zuo and Jones, 1995; etc.]. Additionally, vertical mixing often modifies the CO vertical distributions on the diurnal scale [Kettle, 1994; Doney et al., 1995; Najjar et al., 1995; Gnanadesikan, 1996; Johnson and Bates, 1996].

[3] The magnitudes of CO sources and sinks are, however, very poorly constrained and have become increasingly controversial. The early estimate of Conrad et al. [1982], 4–77 Tg CO-C a⁻¹ (as the sea-to-air gas exchange flux, obviously a lower limit on production), spans a factor of almost twenty. The range of related estimates for various CO sources and/or sinks has widened further in recent years (Table 1b), now implying source strengths ranging over about two orders of magnitude.

[4] Recently, interest in the marine CO cycle has expanded and diversified. CO is a key species for constraining multiprocess models that integrate photochemistry, biology, gas exchange, optics, and mixing to test our

understanding of mixed-layer processes [Kettle, 1994; Doney et al., 1995; Najjar et al., 1995; Gnanadesikan, 1996; Johnson and Bates, 1996; Najjar et al., 2000; Xie et al., manuscript in preparation, 2002]. As the second most abundant carbon-containing product of marine CDOM photochemistry, which is produced in higher yield than all organic compounds combined [Mopper et al., 1991], CO is of interest per se. It has also been used as a proxy to estimate the rates of photoproduction from CDOM of biolabile carbon [Kieber et al., 1989; Miller and Moran, 1997; Moran and Zepp, 1997], and nitrogen compounds [Bushaw et al., 1996]. Since carbon dioxide is a major photoproduct of CDOM, with a yield about 20 times greater than CO [Miller and Zepp, 1995; Gao and Zepp, 1998], its formation may represent a carbon flux larger than that of anthropogenic DIC into the sea [Johannessen, 2000]. CO has also been used as a proxy species in this instance [Johannessen et al., 2000; Mopper

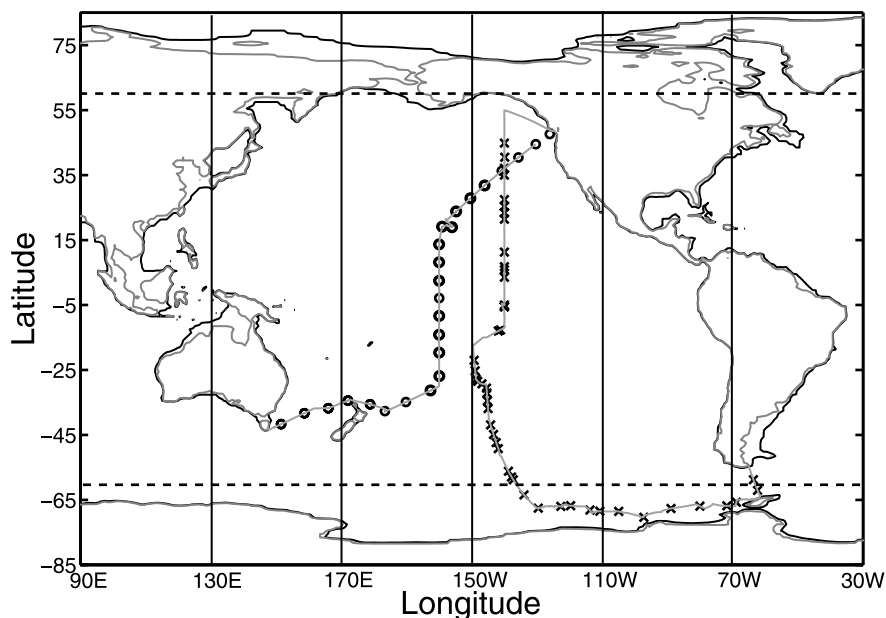


Figure 1. Cruise tracks and sample locations for ACE-1 (circles) (Southern Hemisphere Marine Aerosol Characterization Experiment, R/V *Discoverer*) and RITS-94 (crosses) (Radiatively Important Trace Species, R/V *Surveyor*). See Table 2 for sampling locations. Black contour lines offshore indicate the 200-m isobath. Areas <200 m or greater than 60° north and south (marked with dashed horizontal lines) are excluded from our global “blue-water” estimation. See color version of this figure at back of this issue.

Table 2. Sampling Locations for a_{CDOM} and AQY_{CO} , and k_{CO} ^a

ACE-1 Sampling Sites		RITS-94 Sampling Sites			
Latitude	Longitude	Latitude	Longitude	Latitude	Longitude
47.64	-126.06	44.85	-140.0	-32.10	-145.4
44.5	-130.38	40.50	-139.9	-34.31	-145.2
40.44	-135.7	40.38	-140	-34.50	-145.2
36.3	-140.8	37.11	-140.0	-36.87	-145.0
31.81	-146.05	35.00	-140.0	-41.92	-144.2
27.86	-150.44	28.49	-140	-44.86	-143.3
23.81	-154.78	27.44	-140.0	-45.21	-143.2
18.97	-156.05	25.38	-140.0	-47.37	-142.5
19.12	-159.09	23.41	-140.0	-49.20	-141.9
13.69	-160.01	21.44	-140.0	-55.96	-138.8
8.17	-160	11.27	-140	-56.15	-138.8
2.5	-160	11.27	-140.0	-57.93	-137.8
-2.85	-159.99	6.79	-140.0	-58.79	-137.3
-8.34	-159.98	5.85	-140.0	-63.46	-134.0
-14.14	-160	3.54	-140.0	-67.52	-129.6
-19.66	-159.97	-2.11	-140	-66.98	-122.7
-26.88	-159.94	-4.58	-140.4	-66.78	-119.7
-31.3	-162.65	-4.69	-140.6	-66.43	-131.2
-34.87	-170.19	-4.84	-140.9	-68.10	-113.8
-37.66	-176.64	-5.50	-140.0	-68.47	-110.7
-35.53	178.81	-12.64	-141.2	-68.53	-104.9
-35.58	178.87	-12.64	-141.2	-68.94	-113
-34.4	172.06	-13.00	-141.9	-70.34	-97.2
-36.76	166.01	-22.01	-149.3	-67.64	-88.9
-38.3	158.66	-23.78	-149	-66.91	-80.1
-41.67	151.56	-25.26	-149.0	-66.82	-71.8
		-27.81	-148.7	-65.70	-68.9
		-28.47	-148.2	-62.05	-62.4
		-29.27	-146.9	-58.75	-63.6
		-30.58	-145.5	-58.55	-63.7

^a AQY_{CO} entries are indicated in boldface.

and Kieber, 2000]. Hence, proxy applications of CO may become crucial in extending limited observations of difficult-to-measure carbon dioxide photoproduction to global scales. Thus any evidence that there is a “CO problem” in global budgets, implying that there are important unidentified or misunderstood processes, would be significant in evaluating global biogeochemical cycles other than CO itself.

[5] We report here process studies from two bi-hemispheric blue-water Pacific transects (Figure 1). On the RITS-94 cruise we measured wavelength-specific CO Apparent Quantum Yield (AQY) spectra (AQY_{CO} are moles CO formed per Einstein of light absorbed by CDOM), and also net rate constants of microbial consumption of CO in water from the ship’s pumping system. On ACE-1, microbial CO consumption rate constants were measured using samples from several depths in and below the mixed layer (ML). The ACE-1 data enable us to evaluate the quality of the RITS-94 rate constant measurements (the two ships’ pumping systems are similar), and to examine the extent to which vertical gradients in consumption rate constants and in [CO] cause average ML consumption rates to differ from those extrapolated from near-surface samples.

[6] These data permit (1) readdressing the issue of the open-ocean CO budget by extrapolating the Pacific data, and (2) comparing for the first time independent estimates of CO photoproduction with a sink obtained by adding air-sea CO fluxes [Bates *et al.*, 1995] to microbial loss estimates. With a

few assumptions, known CO sources and sinks can be compared: Do they balance or not?

2. Methods

2.1. CDOM Absorption Spectra

[7] Spectra were measured using freshly collected seawater (Table 2) (usually from the ship’s “clean” underway pumping system, nominally at 5 m [reported here as 4 m to distinguish it from CTD/Niskin samples at ≥ 5 m]) that was gravity-filtered through prerinsed 0.2 μm Nuclepore filters. Spectra were measured in 10-cm quartz cells against a single Milli-Q water reference using an HP 8451 UV-VIS spectrometer, with baseline adjustments described by Green and Blough [1994]. Except for the northernmost (40°N) sample, all CDOM spectra were identical within experimental error; they were averaged to reduce the data noise, and the resultant means were used to obtain the CDOM absorption values used in AQY calculations below (as opposed to using values from log linearized regressions of the spectra). The absorption data are reported as a_{CDOM} (base e, m^{-1}).

2.2. CDOM AQY_{CO} Spectra

[8] AQY_{CO} spectra were obtained using the irradiation system reported by Weiss *et al.* [1995] and Andrews *et al.* [2000]. All work was done at sea on fresh samples (Table 2). Laboratory ambient temperatures ranged from $\sim 30^\circ\text{C}$ in the tropics to below 5°C at high latitudes. Irradiations were performed in 30-cm long, 120 cm^3 quartz cells. Light doses were monitored routinely using an International Light IL1700 radiometer, and calibrated in midcruise using ferrioxalate actinometry [Hatchard and Parker, 1956]. Samples were degassed with CO-free air to minimize their initial [CO] and were transferred in a closed system under CO-free air. [CO] was measured by a headspace method using a Trace Analytical RGA-3 detector [Xie *et al.*, 2002] that was calibrated frequently with a gaseous CO standard supplied by NOAA/PMEL (RITS-94) or a (commercial) gas standard of 1.00 ± 0.03 ppm CO in air (ACE-1). Irradiation of Milli-Q water with equivalent light doses to those incident on seawater samples gave [CO] < 33% of those in seawater (usually much less). Since these signals represent both impurities in the Milli-Q water and any contamination with CO precursors due to sample-handling procedures and apparatus (CO procedure blanks were minimal), they are extreme upper limits to the true blank and were not subtracted. At worst, uncompensated blank effects could thus render AQY data up to 50% high. Irradiation times for accurately measurable [CO] increases varied from 0.25 to 12 hours, with the longer times required at longer wavelengths. Parallel dark samples (degassed seawater held in cells for the irradiation period, then analyzed) increased on average as $[\text{CO}](\text{nmoles}) = 5.7 \times 10^{-2} + 5.6 \times 10^{-3} \times \text{time}(\text{hr})$; they were subtracted as blanks.

2.3. Microbial CO Consumption Rate Constants, k_{CO}

[9] Microbial CO loss rate constants were measured at sites shown in Table 2 in dark incubations over ~ 20 hours (up to 100 hours in cold Antarctic waters). [CO] was measured as described in section 2.2. Since CO loss kinetics are first-order [Jones and Morita, 1984b; Jones and Ama-

dor, 1993; Johnson and Bates, 1996] (and ACE-1 results (not shown)), exponential decays were fitted to the time series data (usually three time points each, with duplicate incubations) to obtain CO loss rate constants, k_{CO} .

[10] This method yields net CO loss rate constants at [CO] slightly below the sample's initial [CO]. The more commonly used ^{14}CO method [Jones, 1991; Jones and Amador, 1993] yields gross rates at [CO] levels considerably above most oceanic [CO] values, but probably in the linear Michaelis-Menton region, hence applicable to calculating k_{CO} values. Three or four incubations indicated net CO production that seemed larger than experimental error; they may indicate true biological/chemical “dark” CO sources, or unknown method or blank effects. Parallel dark incubations of unamended versus ^{14}CO spiked samples would be able to differentiate net versus gross fluxes. Comparison of our CO net bio-consumption rate constants in the dark using the syringe incubation method with those from the ^{14}CO method [Jones, 1991; Jones and Amador, 1993] were carried out once in Florida Bay water and also at BATS, and generally agreed within 20% or better. Differences between incubation-derived rates and in situ rates may also arise due to effects of light on microbial activity [Herndl *et al.*, 1993; Sommaruga *et al.*, 1997]. We measure k_{CO} in darkness, but at BATS we find some light inhibition of CO consumption (light versus dark ^{14}CO method) [Tolli *et al.*, 2000; C. Taylor, personal communication, 2000]. Since ACE-1 samples were obtained in midmorning and incubations began soon thereafter, any light effects that persist into the ensuing dark period affect our rates to some extent. If in situ rates in light are always zero, our rate estimate is high by a factor of 2, but we believe time- and depth-integrated light effects are small: 0–30%, or 0–15% on a 24-hour basis.

2.3.1. ACE-1

[11] Based on the RITS-94 cruise, sampling and incubation methods were improved as detailed by Xie *et al.* [2002]. All samples, mostly from midmorning CTD casts, some with parallel clean-water-system samples, were drawn ($>120\text{ cm}^3$) in dim light in duplicate into acid-cleaned 100 cm^3 all-glass syringes fitted with three-way plastic valves and incubated in very dim light ($\sim 0.1\%$ of UV-free room light intensity). They were subsampled (34 cm^3 with 7 cm^3 prerinses) at three time points over 20–24 hours by coupling the incubation syringe's three-way valve to the three-way valve of a 50 cm^3 analysis syringe that had been preflushed with low-[CO] water. ACE-1 incubation syringes were maintained within 0.3°C of the SST indicated by the ship's 5-m sensor as it approached stations. Samples were generally taken using CTD/rosette (Niskin bottles) in the ML at 5 m, at mid-ML, and at 80–90% of the shallowest visible temperature break; when the ML was $<20\text{ m}$ deep, deeper levels were selected instead or in addition. (The real-time CTD display is too coarse to indicate density gradients that probably inhibit mixing). Incubation syringes were flushed with Nanopure water and soaked for $>15\text{ min}$ every few days to inhibit the buildup of biofilms. [CO] in the syringe bath water was not much above that in syringes, and [CO] values in strongly acidified seawater were stable for 24 hours. The majority of the data regressions have $r^2 > 0.9$; duplicate syringes generally agreed within 22%.

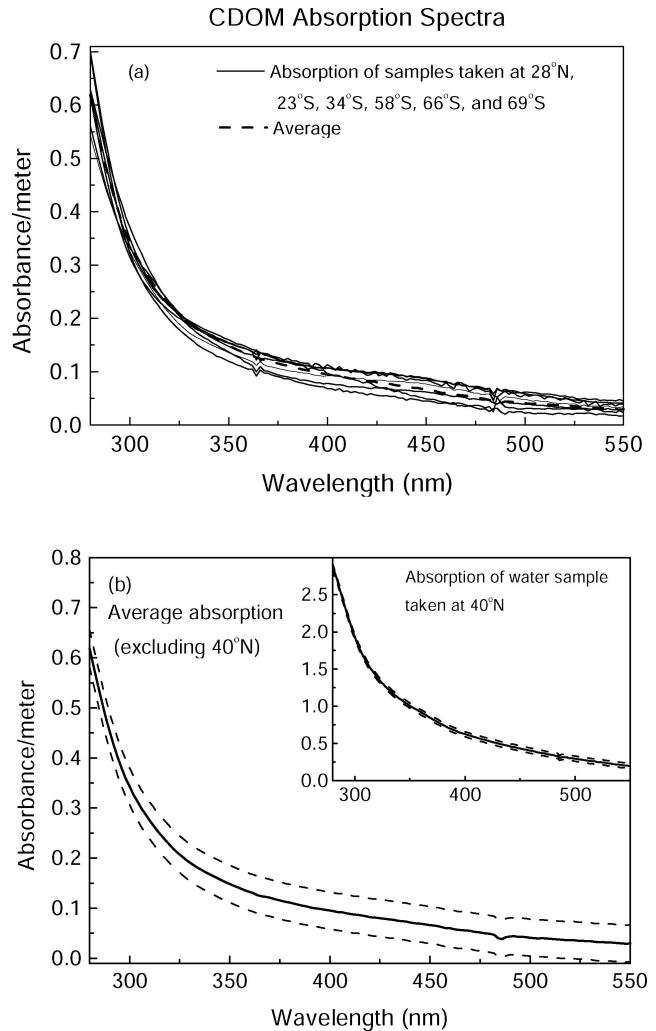


Figure 2. (a) CDOM absorption spectra; (b) averaged spectrum (except 40°N), with “error bars” shown in dashed lines. Inset: 40°N spectrum.

2.3.2. RITS-94

[12] On this first cruise, water was drawn from Niskin bottles through PTFE tubing or from a polycarbonate carboy (both in the manner of dissolved oxygen samples) into 6–8 acid-cleaned, prerinsed 300 cm^3 borosilicate BOD bottles per incubation experiment. The carboy was filled with seawater from the ship's “clean” system (see section 2.2) or with surface water from several casts of a stainless steel bucket with nylon line. The BOD bottles were then incubated in a running seawater bath (usually $\sim 1^\circ\text{C}$ warmer than surface waters) in very dim light and sacrificed sequentially for CO analysis. Incubation temperatures varied up to several degrees from their initial values. Data regressions with $r^2 < 0.7$ were rejected. (The “BOD bottle” method has poor precision, traced to variability in initial [CO] that we attribute to erratic contamination from plastics and other sources [Xie *et al.*, 2002].) This low cutoff for regression coefficients increases the uncertainty of individual k_{CO} values, but since bottles were sacrificed randomly

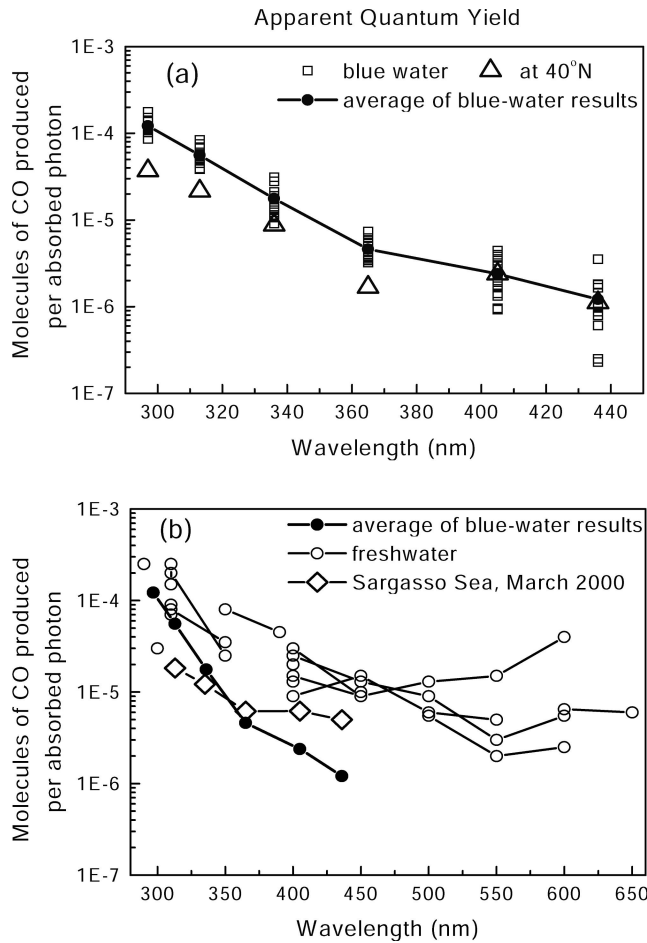


Figure 3. Log linear plots of apparent quantum yield spectra. Apparent quantum yields were calculated as molecules of CO formed per quantum absorbed by CDOM. The uncertainties of the CO production data are typically 15 to 20% at long wavelengths, and smaller at short wavelengths. (a) Apparent quantum yields from different locations indicated by squares, except for 40°N, which is shown as triangles. Solid circles represent the average values that are used in subsequent calculations for the “blue-water” estimation. (b) Averaged data in Figure 3a, the freshwater results from *Valentine and Zepp* [1993], and results of the Sargasso Seawater samples (Xie et al., manuscript in preparation, 2002). Curve fitting of the averaged AQYs from our results gives: $AQY = 9.18 \times 10^{-6} e^{-0.0353(\lambda-360)}$. The parameters are used to extrapolate and interpolate AQYs to all the wavelengths for calculating CO photoproduction in this paper. However, dividing the data into two-segments (see text and Figure 3a) gives better fits: $AQY_{(\lambda < 360\text{nm})} = 5.78 \times 10^{-6} e^{-0.050(\lambda-360)}$, 6.99×10^{-7} , and $AQY_{(\lambda > 360\text{nm})} = 5.24 \times 10^{-6} e^{-0.0229(\lambda-360)}$.

for analysis, no systematic bias to the averaged data should result. Sample water from the ship’s system passed through a pump, while stainless-steel bucket samples at ~6 knots foamed and bubbled extensively, possibly affecting their microbial assemblages’ activities. Cyanide-poisoned samples [Conrad and Seiler, 1980; Conrad et al., 1982] or

samples treated with the nitrification inhibitor N-serve (2-chloro-6-(trichloromethyl) pyridine) in dimethylsulfoxide [Jones and Morita, 1984b] exhibited very small rate constants, including some small CO productions. The cyanide-treated samples behaved most consistently, averaging net [CO] increases of ~3% d⁻¹ (range 0–10% d⁻¹). Since the meaning of k_{CO} values of poisoned samples is unclear, they were not subtracted from unpoisoned-sample k_{CO} values.

3. Results and Discussion

3.1. CDOM Absorption and AQY_{CO} : Results and Spectral Variability

3.1.1. CDOM Absorption Spectra

[13] All a_{CDOM} spectral shapes were very similar, but the water was much more colored at the 40°N site than elsewhere (Figure 2). Due to small signals, in blue waters the absorption due to CDOM is only measurable with moderate precision at the shortest wavelengths and approaches the instrument noise level at ~400 nm. Additionally, the unavailability of high-purity feed water for the Milli-Q system on R/V *Surveyor* led us to compare all samples to a single sealed cell of Milli-Q water prepared in Seattle. Confidence in this reference and in these data is enhanced by the similarity of our spectra in the Antarctic region (near/at the end of the cruise) to those reported in a similar season and region by *Yocis et al.* [2000].

3.1.2. AQY_{CO} Spectra

[14] The principal experimental uncertainty in AQY_{CO} spectral data lies not in the [CO] measurements, but in the CDOM absorption coefficients, as discussed above. Sam-

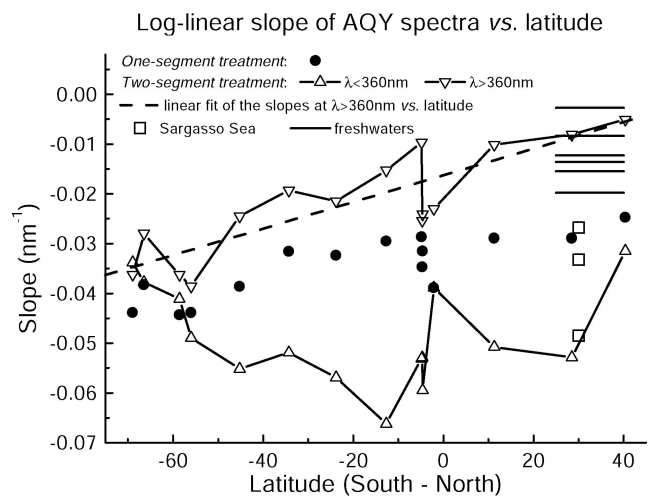


Figure 4. Log linear slopes of AQY_{CO} versus latitude. Measurements from freshwater [Valentine and Zepp, 1993] and Atlantic water (Xie et al., manuscript in preparation, 2002) samples are also included for comparison. The negative values indicate that photoproduction is more efficient at short wavelengths; small absolute values indicate that production at longer wavelengths becomes relatively more significant. In the two-segment treatment, the log linear slopes of the AQYs beyond 360 nm are more negative toward south. See Figure 3 caption for equations defining one- and two-segment slopes.

Table 3. Pacific and Global CO Source and Sink Estimates From AQY_{CO} and k_{CO} Data in This Paper^a

Region	Source (+), Tg CO-C a ⁻¹ , (Photochemical Production)	Sink (-), Tg CO-C a ⁻¹ , (Microbial Consumption)		
		Cruise	a	b
Pacific	27	ACE-1	-26 ± 15	-22 ± 12
		RITS-94	-15 ± 6	-12 ± 5
Global	50 ± 10	ACE-1	-45 ± 26	-37 ± 22
		RITS-94	-25 ± 10	-21 ± 9
Weighted Global Average	(N/A)	ACE-1 (n = 213) RITS-94 (n = 87)	-38 ± 21	-32 ± 18

^aMethod “a” gives surface [CO] from *Bates et al.* [1995], assuming mixed layer [CO] = surface [CO]; method “b” gives surface [CO] calculated from the [CO] depth profiles measured at time zero of the incubation experiments. We consider method b to be the best estimate. The ± values are derived propagation of estimated measurement errors. See Figure 9 for estimated total ranges of values.

ples from central gyres, the equatorial upwelling, the southern ocean, and the North and South Pacific (with very different riverine input/ocean area ratios) are all represented (Figure 1, Table 2), as is the late fall/early spring seasonal contrast. These varied samples might be expected to exhibit revealing geographical variations in their photophysical and photochemical properties, since there are at least two pools of CDOM: marine [*Siegel and Michaels, 1996; Hedges et al., 1997; Opsahl and Benner, 1997; Vodacek et al., 1997; Nelson et al., 1998*] and terrestrial [*Kalle, 1966; Højerslev, 1982; Mopper et al., 1991; Valentine and Zepp, 1993; Amon et al., 1999*]. There are also multiple mechanisms by which CDOM generates CO [*Redden, 1982; Gao and Zepp, 1998*]; their relative efficiencies and contributions may vary. However, the AQY spectra, shown on a logarithmic scale as a function of wavelength in Figure 3a, are quite uniform. The striking exception at 40°N is mainly driven by the absorption difference (Figure 2), giving AQYs about ten-fold lower than the other sites. Obviously, more samples from such regions are needed.

[15] Closer inspection reveals a large-scale AQY_{CO} trend: spectral slopes differ at long and short wavelengths, as shown in Figure 3a by the two roughly linear segments. Separately analyzing the slopes in these two regions reveals a systematic N–S trend in the long-wavelength slopes and also shows that the anomalous 40°N site’s slope at $\lambda > 360$ nm resembles the slope of terrestrial CDOM (Figures 3b and 4). There are thus subtle a_{CDOM} and/or AQY_{CO} differences, mainly evident on the interhemispheric scale, rather than the regional signatures (gyres, upwelling) that had been expected. These observations defy unique interpretation, however, because the data convolute several factors: (1) interhemispheric differences, (2) seasonality, (3) temperature effects (AQYs were measured at laboratory temperatures differing from SST, except in midlatitudes), and (4) effect of regional variations in a_{CDOM} on AQY_{CO} (since an average a_{CDOM} spectrum was used to calculate AQYs).

[16] The similarity of the AQY_{CO} spectral slope at 40°N to that for terrestrial CDOM, together with the larger riverine inputs in the Northern versus Southern Hemisphere, suggest the terrestrial/marine CDOM input ratio is a plausible slope-controlling variable. However, most riverine CDOM discharges in the Atlantic and Arctic rather than the Pacific [*Opsahl and Benner, 1998; Amon et al., 1999*], and near the surface, interhemispheric water exchange is a slow process. Hence terrestrial influences in the Pacific may be relatively small, but should yield a relatively sharp

discontinuity across the equator. No such discontinuity is clear in the data.

3.1.3. Blue-Water Photochemical CO Production

[17] Photochemical CO production can be described as the areal sum of the products of sunlight absorbed by CDOM and its AQY_{CO} over all relevant wavelengths (300–800 nm):

$$\sum_{\text{ocean area}} \int_{300}^{800} (\text{attenuation factor} \times \text{insolation} \times [1 - e^A] \times \text{AQY}_{\text{CO}}) d\lambda,$$

in which A is the absorption of light by CDOM in the water column. Both A and AQY_{CO} are functions of wavelength λ .

[18] Cloud-free spectral insolation data of *Leifer* [1988] and the averages of the measured absorption and AQY_{CO}, excluding those at 40°N, are used to calculate production. The spectral insolation data are seasonal averages in 10° latitude bands, excluding coastal areas (depth <200 m). We assume that about 20% of the total insolation is reflected by clouds and about 30% absorbed by such non-CO producing chromophores as water and particulate material [*Nelson et al., 1998*]; the average non-CDOM absorption at 440 nm is about 50% (*D. Siegel, personal communication, 2001*), but decreases at shorter wavelengths. Therefore, the attenuation factor in the above equation is 0.7. The average AQY_{CO} data are fitted to a straight line on a log linear scale to interpolate and extrapolate AQY_{CO} to the desired wavelengths (300–800 nm), or are fitted to two linear segments as shown in Figure 3a. (See Figure 3 caption for the equations.) The resulting total CO productions using either method are similar. The difference is the partitioning of the productions between the short and long wavelengths (Figure 3a). Because we focus on the total CO photochemical production over all wavelengths in this paper, we show the results of the one-segment treatment in Table 3 for the Pacific and global (60°S–60°N) CO photochemical production rates. In this treatment, 45% of CO forms at 300 to 340 nm, 52% at 340 to 450 nm, and 3% at wavelengths above 450 nm. The global rate, 50 ± 10 Tg (uncertainty from propagation of errors only) probably lies in our conservatively estimated range of 30–70 Tg CO-C a⁻¹.

[19] These estimates are much smaller than almost all other published photochemical CO source estimates (Table 1b versus Table 3, recalling that CO formation must equal or exceed outgassing). Using our AQY_{CO} data set along with global insolation, cloudiness, and an a_{CDOM} field derived from ocean color data, *Siegel* [2001] also recently

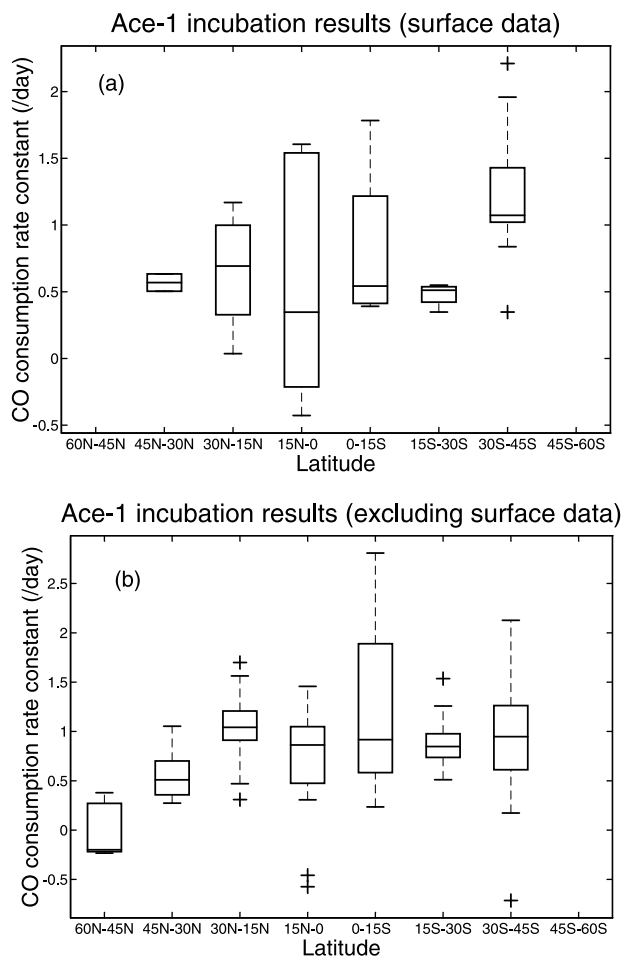


Figure 5. Boxplot of ACE-1 microbial decay rate constants, k_{CO} , for (a) surface (5 m) CTD samples and (b) mixed-layer (and sometimes deeper) samples. The boxes have lines at the lower quartile, median, and upper quartile values. The whisker lines extending from each end of the box show the range of the data, except a few points considered outliers (pluses).

estimated a photoproduction of ~ 30 Tg CO-C a^{-1} globally, equal to our minimum estimate. Possible deficiencies in our data that might greatly affect these production estimates include (1) AQY_{CO} at >450 nm is unconstrained by data; there is much insolation there, and terrestrial CDOM produces CO to >600 nm [Valentine and Zepp, 1993] (Figure 3b), (2) if a_{CDOM} data were systematically in error at 365–436 nm, where the signal-to-noise ratio is poor, then our AQY_{CO} values are erroneous, and (3) AQY_{CO} values at our sites might be lower than in regions more influenced by terrestrial inputs (Atlantic, North Indian, and Arctic Oceans), or with different ecosystem biogeochemistry that somehow affects the relevant properties of CDOM. For example, regional variations in limiting nutrients, such as N, P, and Fe, might affect the nature of marine CDOM. Also, our samples are likely contaminated with Fe at the pM-nM level; at least in acidic freshwater rivers, Fe enhances CO photo-production and CDOM photobleaching

[Gao and Zepp, 1998]. However, our estimated CO production per unit area in the Pacific is very similar to production profiles measured in situ by suspending samples on “optical buoys” (C. Taylor et al., manuscript in preparation, 2002) in the Atlantic near BATS (N. B. Nelson et al., Light energy control of photochemistry in the Sargasso Sea: Estimates of photochemical quantum yield by optical closure, manuscript in preparation, 2002) (hereinafter referred to as Nelson et al., manuscript in preparation, 2002). These experiments include the effects of all wavelengths, and do not use a_{CDOM} or AQY_{CO} data. Also, addition of Fe or of the Fe chelator DFOM had little effect ($\pm 30\%$) on these “optical buoy” results [Goldstone, 2002].

[20] Despite the complexities cited above, this “optical buoy” comparison suggests that our Pacific data are roughly correct and that the world ocean does not vary greatly in the factors controlling CO photoproduction, apart from coastal regions, consistent with the idea that most terrestrially derived photoreactive CDOM is processed rather quickly photochemically [Vodacek et al., 1997; Andrews et al., 2000] and biologically [Kieber et al., 1989; Miller and Moran, 1997; Moran and Zepp, 1997] so that relatively little reaches central gyres.

3.2. Blue-Water Microbial Net CO Sink: k_{CO}

3.2.1. ACE-1 Data

[21] The latitude-binned CO microbial decay rate constants for the surface (5 m) CTD samples are shown in Figure 5a, with deeper values (occasionally below) the ML in Figure 5b. The depth-binned data are also shown in Figure 6. These k_{CO} data (0–60 m, usually three depths in the ML) range from -0.5 to 2.9 d^{-1} (here negative numbers indicate increases in [CO]; fewer than 4% of the k_{CO} values were negative). In summary, 72% of the values lie between 0.5 and 1.5 d^{-1} , with the median being 0.84 d^{-1} and the average 0.86 d^{-1} . On average there is about twice the variability in k_{CO} values measured in pumping-system

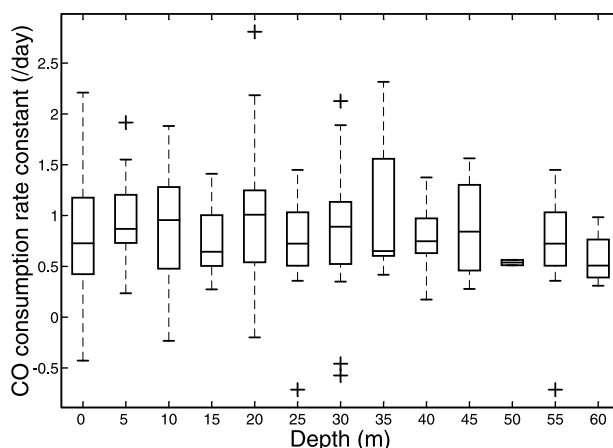


Figure 6. ACE-1 microbial decay rate constants, k_{CO} , binned by sample depth. Again, the boxes have lines at the lower quartile, median, and upper quartile values. The whisker lines extending from each end of the box show the range of the data, except a few points considered outliers (plus signs).

Table 4. Microbial CO Loss Rate Constants, day⁻¹

Sample Type	Northern Hemisphere			Southern Hemisphere			Southern Ocean ^a		
	Mean	n	Std Dev	Mean	n	Std Dev	Mean	n	Std Dev
RITS94 (4 m Pump)	0.69	1	0.31	0.52	3	0.35	0.09	1	0.11
ACE-1 (Pump System)	0.60	1	0.57	1.01	2	0.55			
ACE-1 (5 m)	0.86	1	0.32	0.99	1	0.41			
ACE-1 (top 3 depths)	0.70	3	0.41	1.01	2	0.45			

^aNote that these values are not used in our estimate (Table 3; Figure 1).

samples as in CTD/Niskin samples (Table 4). The intra-cruise k_{CO} variability is, however, larger than the difference in the cruise means; the mean pump-system/Niskin k_{CO} ratio for comparable samples is only 0.7 for the Northern Hemisphere and 1.02 for the Southern Hemisphere. An examination of individual profiles (not shown) also confirms there is little mean vertical gradient in k_{CO} . (A detailed k_{CO} profile at a station with unusually complex T-S structure is shown in Figure 7.) At the shallow depths chosen to cover the deeper of the ML or the CO photoproduction zone, the ML and uppermost thermocline thus appear homogenous with respect to k_{CO} . However, there was often a [CO] gradient, with lower concentrations at greater depths (note that uniform k_{CO} profiles do not imply uniform CO loss rate profiles unless [CO] is also uniform).

3.2.2. RITS-94 Data

[22] Method and sampling constraints on RITS-94 (see section 2.3) yielded noisier data than those of ACE-1's CTD samples; since no other data exist in these regions and the comparisons above suggest they are valid, we report them in

Table 4. As in ACE-1, despite the wide range of oceanic regimes traversed, and contrary to the preconceptions motivating us to make these measurements, there was generally little systematic trend to the rate constants. However, as SST dropped precipitously below 10°C in southerly latitudes, k_{CO} values dropped five-fold or more, averaging ~ 0.1 d⁻¹. Due to blank issues, long incubations, and high scatter in data, these values merely establish a conservative limit on the average k_{CO} of <0.2 d⁻¹ for this region.

[23] Strikingly, surface water [CO] in the southern ocean in austral summer is more than twice as high as in any other region or season [Bates *et al.*, 1995]. Since our AQY_{CO} values there were typical of other regions and insolation was well below average due to low sun angles and extensive fog, CO photo-production is expected to be low. Low production alone lowers [CO]; high [CO] thus requires either a new CO source or less active CO sink(s). High Antarctic [CO] values can thus be understood qualitatively as resulting from a cycle in which a large weakening of CO sinks outweighs a smaller weakening in photoproduction,

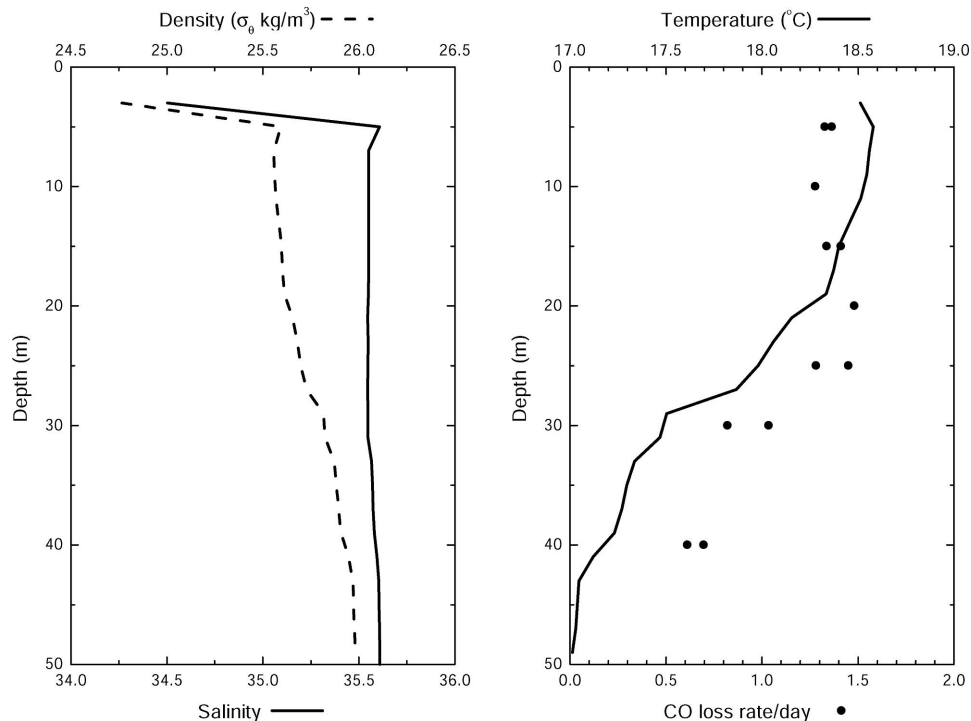


Figure 7. Detailed vertical profile of k_{CO} in a shallow, structured mixed layer (latitude 31°17.99', longitude: 162°39.01').

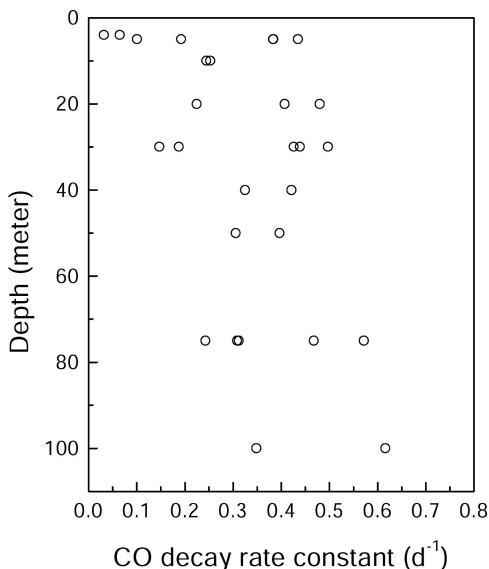


Figure 8. Profiles of microbial k_{CO} decay constants by the incubation method at the RITS-94 station ($5.5^{\circ}S$) that was modeled by *Johnson and Bates* [1996]. Mean = $0.33 d^{-1}$.

although variations in vertical mixing probably also play a role by varying the depth over which CO mixes down and is diluted.

[24] The RITS-94 data also permit a comparison of incubation-derived rates with an independent method, the in situ time series CO nighttime inventory loss method of *Johnson and Bates* [1996]. Unfortunately, this comparison occurred at an atypical site at which [CO] was unusually high and the CO diurnal cycle was unusually weak. *Johnson and Bates* [1996] estimated by modeling that the biological rate constant there was $0.09 d^{-1}$, with 60–90% statistical fit uncertainty, and an additional 50% uncertainty in the (large) gas-exchange term that was subtracted from the total nighttime CO loss rate to obtain the biological oxidation term. Our profile measurements at this station showed great variability (Figure 8), averaging $\sim 0.3 d^{-1}$, in poor to fair quantitative agreement, but qualitatively confirming their result. These low values suggest that this station is an example from the tropics in which high [CO] results mainly from a relatively slow biological sink rather than from elevated CO photo-production, as the Antarctic data also suggested. This inter-comparison thus seems inconclusive, neither validating nor condemning our method. A less direct comparison can also be made with the RITS93 in situ time series study of *Johnson and Bates* [1996]. This station exhibited more typical CO dynamics, and its modeled k_{CO} of $0.46 d^{-1}$ is within 1 standard deviation of six of the eight means we report in Table 4. Given the added uncertainty in the gas-exchange term they subtracted, this comparison is satisfactory.

3.2.3. Global Blue-Water Microbial Consumption

[25] The rate constants presented above are the first k_{CO} survey of large blue water areas. ML gross rate constants reported for coastal and riverine-influenced waters by the ^{14}CO method tend to be considerably higher, though Caribbean blue-water values away from the Orinoco Plume

were lower ($\sim 0.2\text{--}0.5 d^{-1}$) [*Jones and Amador*, 1993], as were some in the southern NW Atlantic [*Jones*, 1991]. However, estimates in the N. Atlantic ($\sim 32^{\circ}N$, $64^{\circ}W$) in summer and spring from modeling poisoned versus unpoisoned in situ “optical buoy” data (Nelson et al., manuscript in preparation, 2002) and from ^{14}CO method studies in dark and light conditions [*Tolli et al.*, 2000] also lie in the $0.5\text{--}1.5 d^{-1}$ range. As in the case of the AQY_{CO} data, available information is thus consistent with the simple assumption that our Pacific microbial consumption data are roughly representative of other blue-water sites.

[26] We have estimated the blue-water Pacific microbial CO sink ($60^{\circ}N\text{--}60^{\circ}S$, water column depths >200 m), and from it extrapolated an analogous global sink, using either RITS-94 data only or ACE-1 data only. The microbial CO consumption rates are calculated as follows: (1) the measured microbial CO consumption rate coefficients are grouped and averaged in 15° latitude bands for both ACE-1 and RITS-94 cruises; (2) the area of the ocean is obtained excluding the area where the bottom depth is shallower than 200 m; (3) seasonal mean mixed-layer depth is taken from Levitus94 [*Conkright et al.*, 1994]; and (4) the area integral of the mixed-layer depth gives the volume of water in which [CO] throughout the mixed-layer is either assumed to be the same as the surface [CO] and the values are taken from *Bates et al.* [1995, Table 2] or calculated from the depth profiles of [CO] measured at time zero of the incubation experiments. Since [CO] usually decreases with increasing depth in the ML in daytime, the first assumption overestimates [CO] in the mixed-layer and leads to higher CO consumption rates. It should also be noted that a small fraction of the k_{CO} data in our ML estimate are actually from below the ML.

[27] In summary, factors contributing to potential systematic errors in these microbial sink estimates include: incubation effects, photo-inhibition effects, overestimation or underestimation of deeper [CO] due to temporal bias (most samples were taken at local midmorning on ACE-1), overestimation of the diurnally effective ML depth by using seasonal values, and using net instead of gross rates. This last point is more a matter of terminology than of substance in view of the absence of evidence for nonphotochemical CO production in marine samples. In our opinion, most of these potential effects would tend to bias our sink estimate to the high rather than to the low side.

[28] Weighting ACE-1 and RITS-94 data equally by the number of observations and using method b (above and Table 3) gives a propagation-of-error best-estimate microbial sink of $32 \pm 18 Tg CO-C a^{-1}$. For budgets, we adopt a subjective but conservative range: $10\text{--}60 Tg CO-C a^{-1}$. Although the CO microbial sinks estimated from the two cruises overlap, in view of the better samples and more precise technique of ACE-1, those data should arguably be weighted more heavily (slightly raising the sink estimate).

3.2.4. Total Global Blue-Water CO Sink

[29] The CO gas exchange flux has been estimated by *Bates et al.* [1995] as $\sim 5.5 Tg CO-C a^{-1}$ (0.3 from the $60^{\circ}\text{--}75^{\circ} N/S$ bins excluded by us). However, a reviewer of this paper has pointed out that this estimate is based on [CO] data from 4–5 m and that there may be different, higher

[CO] near the sea surface. Although there are few data addressing this point, at BATS in summer (low wind) we used an in situ pumping system [Donoghue *et al.*, 2001] coupled to an automated system [Xie *et al.*, 2001] to sample water at 1- and 8-m depths, and found no detectable [CO] gradient (<10%) (Xie *et al.*, manuscript in preparation, 2002).

[30] Summing Bates *et al.*'s [1995] outgassing of 5.5 Tg CO-C a⁻¹ and our value for microbial consumption of 32 ± 18 Tg CO-C a⁻¹ yields a blue-water sink of 38 ± 20 Tg CO-C a⁻¹; again we adopt a more conservative range, 13–60 Tg CO-C a⁻¹. (The small area south of 60°S and k_{CO} values there, <0.2 d⁻¹, suggest that the southern ocean's microbial sink is far below our uncertainties.) Despite its high summer [CO], excluding the southern ocean thus makes little difference. The Arctic is ignored as largely ice-covered, <200 m deep, or both.

[31] Comparing the best estimates for the two sinks suggests that globally most CO (~86%) is cycled internally by microbial processes. Extreme errors (half the microbial sink, twice the outgassing) would still leave the microbial term dominant. Thus, the oceanic biogeosphere strongly buffers the CO partial pressure over the sea. The biological function of CO consumption (oxidation to carbon dioxide, based on ¹⁴CO results; [Jones and Morita, 1984a, 1984b; J. Tolli, personal communication, 2000]) and the active microbial populations are little known. Based in part on strong “N-Serve” inhibition, Jones has argued that nitrifiers are the active oxidizers; our experiments confirm this inhibition (although the effect may not be nitrifier-specific (B. B. Ward, personal communication, 1986)). A nitrification sink suggests a “signature” in crossing from central gyres to equatorial upwelling, since presumably there is a large shift in the roles of new vs. regenerated production, with corresponding differences in ammonium cycling rates, nitrifier activities, and hence (simplistically) CO consumption rates. On the other hand, the large-scale distribution of microbial activity, a conceivable alternative proxy for CO-oxidizing activity, appears to be relatively invariant [Carlson *et al.*, 1996], compared to primary productivity variations [Walsh, 1998].

3.3. Blue-Water and Coastal CO Sources, Sinks, and Inventory

[32] A complete blue-water budget requires accounting for sources, sinks, and changes in the CO inventory of the waters considered (here, the deeper of ML or CO-photo-production zone, 33–50% of the 1% PAR level). The ML inventory (~2 × 10¹¹ g C for an average 40 m depth and the [CO] data of Bates *et al.* [1995]) is negligible in comparison to annual turnover, as expected since CO turns over rapidly (< a few days). The sum of CO sources should thus equal the sum of CO sinks. In fact, either estimated source derived from our AQY_{CO} data, (50 or 30 [Siegel, 2001] Tg CO-C a⁻¹) matches the estimated sink within uncertainties. The almost perfect concordance of the sink with the averaged source, 38 versus 40 [Siegel, 2001] Tg CO-C a⁻¹, is striking, if probably fortuitous. These are independent source and sink estimates (both depend on analytical [CO] standards that are expected to be accurate to better than 20%, probably much better). This source-sink

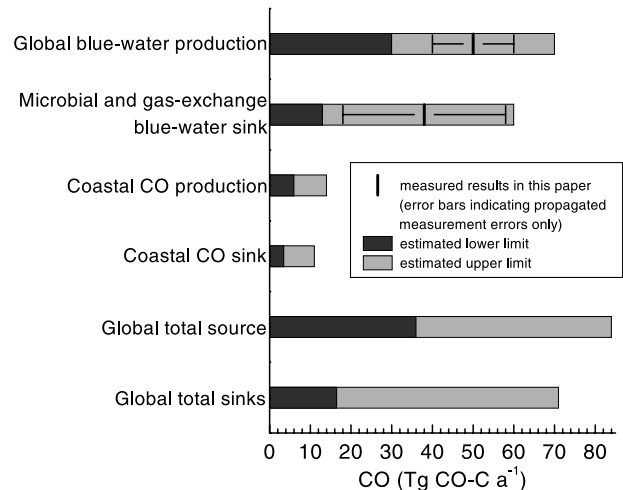


Figure 9. Summary of CO budget term estimations. See text for assumptions and databases. Literature values are summarized in Table 1b.

concordance thus lends credence to the estimates and their underlying data, and requires that if any major unrecognized sources and sinks exist, they must balance fortuitously. While Occam's razor suggests that they probably do not exist, the substantial uncertainties in these estimates certainly leave room for additional undetected sources and/or sinks.

[33] The total marine CO flux, including coastal waters, is also of interest, and is conceptually a more cleanly delineated compartment than is the fuzzy-edged blue-water regime. On the sink side, the (largely coastal) Arctic and other coastal waters are very poorly constrained. River-influenced low- and intermediate-latitude waters probably consume CO several times faster per unit area than does blue-water (Jones and Amador's [1993] median ML value for blue-water being 0.45 d⁻¹ (n = 7), and 3.4 d⁻¹ for coastal waters (n = 24)). In arid coastal regimes, our Southern California (CALCOFI) three-cruise data show very modest k_{CO} and [CO] increases inshore versus offshore (O. C. Zafriou, unpublished data, 1997). Thus a reasonable estimate for the coastal microbial CO sink is 1.5–4.5 times the k_{CO} values of blue-water, times the (unknown) coastal/blue-water [CO] ratio, surely >1, giving >(3.5–11) Tg CO-C a⁻¹, with no strong upper limit.

[34] A rough coastal CO source estimate can be made assuming there are two components: (1) reactive terrestrial DOM inputs, whose photo-labile CDOM component seems to be largely photoprocessed locally in coastal regions [Vodacek *et al.*, 1997; Andrews *et al.*, 2000], and (2) a productivity-related component like the blue-water CDOM cycle, scaled up to reflect higher coastal productivity, but ignoring any coast-specific benthic or ecosystem-specific effects. A very conservative upper bound on the photolabile terrestrial CDOM term is 100% of the estimated terrestrial DOM input to the oceans, 0.2 Tg C per year [Sarmiento and Sundquist, 1992] times the ratio of CO to CO₂ in the products, 0 to 1/15–1/20 [Miller and Zepp, 1995], or ~0.01 Tg CO-C a⁻¹. This is ~1/200 of the blue-water

flux in 7% of the area, enhancing the reactivity on an area basis relative to blue waters by <10%. The “directly terrestrial” CO input thus appears to be truly negligible in budgeting, although within and near river plumes there can be large effects.

[35] The second coastal component, productivity-stimulated CDOM production, and resultant increased CO production, is more complex. Although marine CDOM is presumably formed in proportion to primary productivity, hence at ~ 3 – 4 times the blue-water rate [Walsh, 1998], if its AQY_{CO} is the same as we measured, this CDOM may not all be photolyzed coastally before being exported to adjacent mixing regions, which we likely undersampled. We will treat this CDOM as though it forms and photolyzes coastally. There is one AQY_{CO} data set [Ziolkowski, 2000] that indicates values several times higher than our blue-water data. This coastal source is thus plausibly $\sim 3 \times 0.07 \times 50 = 10$ Tg CO-C/yr, implying a coastal plus blue-water CO cycle of ~ 50 Tg CO-C a⁻¹.

[36] In summary, it is difficult to rationalize a global marine CO cycle outside the extreme range ~ 15 – 80 Tg CO-C a⁻¹ without invoking new processes or very different biogeochemical dynamics, which are certainly possible but not supported by relevant evidence. We believe that other, much larger estimates (Table 1b) are most likely in error; none is derived from blue-water AQY or in situ photochemical CO production measurements. Several can be easily understood as extrapolations of terrestrial AQY_{CO} data over oceanic areas, insolation conditions, etc. Our data now show that the implicitly assumed coastal and blue-water quantitative similarities do not exist (Figure 3b), at least at 300–365 nm (the peak production wavelength region), in the Pacific and southern oceans. Other large values, especially those by Zuo and Jones [1995] and by Erickson [1989], are harder to understand. Jones’ site might be influenced by Amazon and Orinoco outflows, but probably not substantially. Erickson’s estimate for out-gassed CO, scaled to the Atlantic observations of Conrad *et al.* [1982] by means of remotely sensed chlorophyll fields, is indirect but seems reasonable in conception.

[37] We summarize the data interpretations and coastal speculations made above in Figure 9. The other estimates (except the sea-air flux of Bates *et al.* [1995]) in Table 1b lack the directness, coverage, or consistency checks comparable to this work. However, our spatiotemporal coverage is still woefully thin; with no k_{CO} or AQY_{CO} measurements at all in the South Atlantic, Indian or Arctic Oceans, and only a few points in the North Atlantic near BATS. Compared to their variability and likely extents, river-influenced coastal regions are a data-vacuum. As can be seen above, coastal areas are at present simply battleground for very different speculative extrapolations seaward from the land (e.g., selected entries in Table 1b) and landward from blue-water (above). While it seems most plausible to us that on average coastal waters more closely resemble modified blue-waters than modified river waters, only data will tell.

[38] **Acknowledgments.** We thank RITS-94 Chief Scientists Tim Bates and Jim Johnson of NOAA/PMEL, and the captain and crew of R/V *Surveyor*, for assistance on RITS-94 and for discussions, T. Jones and

C. Taylor for comparison of k_{CO} methods, and Richard Zepp for further discussions. Drs. John Hedges, John Milliman, and Steve Opsahl also advised about riverine inputs. C. Chandler assisted in data reduction. B. Voelker, R. Najjar, and three anonymous reviewers provided critical, constructive comments. OCZ acknowledges an NRC Associateship at US-EPA (Athens, GA). This work was supported by NSF grants OCE-915608 and OCE94-817214, ONR N00014-91-1258, and NASA NAGW-2431, WHOI contribution 10160.

References

- Amon, R. M. W., S. Opsahl, and R. Benner, Major flux of terrigenous dissolved organic matter through the Arctic Ocean, *Limnol. Oceanogr.*, **44**, 2017–2023, 1999.
- Andrews, S. S., S. Caron, and O. C. Zafriou, Photochemical oxygen consumption in marine waters: A major sink for colored dissolved organic matter?, *Limnol. Oceanogr.*, **45**, 267–277, 2000.
- Bates, T. S., K. C. Kelly, J. E. Johnson, and R. H. Gammon, Regional and seasonal variations in the flux of oceanic carbon monoxide to the atmosphere, *J. Geophys. Res.*, **100**(D11), 23,093–23,101, 1995.
- Bullister, J. L., N. L. Guinasso, and D. R. Schink, Dissolved hydrogen, carbon-monoxide, and methane at the CEPEX site, *J. Geophys. Res.*, **87**(C3), 2022–2034, 1982.
- Bushaw, K. L., R. G. Zepp, M. A. Tarr, D. SchulzJander, R. A. Bourbonniere, R. E. Hodson, W. L. Miller, D. A. Bronk, and M. A. Moran, Photochemical release of biologically available nitrogen from aquatic dissolved organic matter, *Nature*, **381**(6581), 404–407, 1996.
- Carlson, C. A., H. W. Ducklow, and T. D. Sleeter, Stocks and dynamics of bacterioplankton in the northwestern Sargasso Sea, *Deep Sea Res., Part II*, **43**(2–3), 491–515, 1996.
- Conkright, M. E., S. Levitus, and T. P. Boyer, *World Ocean Atlas 1994*, U.S. Dep. of Commerce, Natl. Oceanic and Atmos. Admin., Natl. Environ. Satellite, Data, and Inf. Serv., Gov. Printing Off., Washington, D. C., 1994.
- Conrad, R., and W. Seiler, Photo-oxidative production and microbial consumption of carbon-monoxide in seawater, *FEMS Microbiol. Lett.*, **9**(1), 61–64, 1980.
- Conrad, R., and W. Seiler, Utilization of traces of carbon-monoxide by aerobic oligotrophic microorganisms in ocean, lake and soil, *Arch. Microbiol.*, **132**(1), 41–46, 1982.
- Conrad, R., W. Seiler, G. Bunse, and H. Giehl, Carbon monoxide in seawater (Atlantic Ocean), *J. Geophys. Res.*, **87**(C11), 8839–8852, 1982.
- Doney, S. C., R. G. Najjar, and S. Stewart, Photochemistry, mixing and diurnal cycles in the upper ocean, *J. Mar. Res.*, **53**, 341–369, 1995.
- Donoghue, T., O. C. Zafriou, and C. D. Taylor, Retractable surface-following sampler, *Mar. Tech. Soc.*, **35**(2), 29–35, 2001.
- Erickson, D. J., III, Ocean to atmosphere carbon monoxide flux: Global inventory and climate implications, *Global Biogeochem. Cycles*, **3**, 305–314, 1989.
- Gammon, R. H., and K. C. Kelly, Photochemical production of carbon monoxide in surface waters of the Pacific and Indian oceans, in *Effects of Solar Ultraviolet Radiation of Biogeochemical Dynamics in Aquatic Environments*, edited by N. V. Blough and R. G. Zepp, Woods Hole Oceanogr. Inst., Woods Hole, Mass., 1990.
- Gao, H., and R. G. Zepp, Factors influencing photoreactions of dissolved organic matter in a coastal river of the Southeastern United States, *Environ. Sci. Technol.*, **32**, 2940–2946, 1998.
- Gnanadesikan, A., Modeling the diurnal cycle of carbon monoxide: Sensitivity to physics, chemistry, biology, and optics, *J. Geophys. Res.*, **101**(C5), 12,177–12,191, 1996.
- Goldstone, J. V., Direct and indirect photochemical reactions of chromophoric dissolved organic matter: Roles of reactive oxygen species and iron, Ph.D. thesis, Woods Hole Oceanogr. Inst.-Mass. Inst. of Technol. Joint Program in Oceanogr., Woods Hole, Mass., 2002.
- Green, S. A., and N. V. Blough, Optical absorption and fluorescence properties of chromophoric dissolved organic matter in natural waters, *Limnol. Oceanogr.*, **39**, 1903, 1994.
- Hatchard, C. G., and C. A. Parker, A new sensitive chemical actinometer, 2, Potassium ferrioxalate as a standard chemical actinometer, *Proc. R. Soc. London, Ser. A*, **235**(1203), 518–536, 1956.
- Hedges, J. I., R. G. Keil, and R. Benner, What happens to terrestrial organic matter in the ocean?, *Org. Geochem.*, **27**(5–6), 195–212, 1997.
- Herndl, G. J., G. Muller-Niklas, and J. Frick, Major role of ultraviolet-B in controlling bacterioplankton growth in the surface layer of the ocean, *Nature*, **361**, 717–719, 1993.
- Højerslev, N., Yellow substance in the sea, in *The Role of Solar Ultraviolet Radiation in Marine Ecosystems*, edited by J. Calkins, pp. 263–281, Plenum, New York, 1982.

- Johannessen, S. C. H., A photochemical sink for dissolved organic carbon in the ocean, Ph.D. thesis, 171 pp., Dep. of Oceanogr., Dalhousie Univ., Halifax, N. S., Canada, 2000.
- Johannessen, S., L. Ziolkowski, and W. Miller, Comparison of photochemical production rates of carbon monoxide and dissolved inorganic carbon in the ocean, paper presented at Pacificchem 2000, Am. Chem. Soc. Pacificchem, Honolulu, Hawaii, 2000.
- Johnson, J. E., and T. S. Bates, Sources and sinks of carbon monoxide in the mixed layer of the tropical South Pacific Ocean, *Global Biogeochem. Cycles*, 10(2), 347–359, 1996.
- Jones, R. D., Carbon monoxide and methane distribution and consumption in the photic zone of the Sargasso Sea, *Deep Sea Res.*, 38(6), 625–635, 1991.
- Jones, R. D., and J. A. Amador, Methane and carbon-monoxide production, oxidation, and turnover times in the Caribbean Sea as influenced by the Orinoco River, *J. Geophys. Res.*, 98(C2), 2353–2359, 1993.
- Jones, R. D., and R. Y. Morita, Effects of various parameters on carbon-monoxide oxidation by ammonium oxidizers, *Can. J. Microbiol.*, 30(7), 894–899, 1984a.
- Jones, R. D., and R. Y. Morita, Effect of several nitrification inhibitors on carbon-monoxide and methane oxidation by ammonium oxidizers, *Can. J. Microbiol.*, 30(10), 1276–1279, 1984b.
- Kalle, K., The problem of gelbstoff in the sea, *Oceanogr. Mar. Biol. Ann. Rev.*, 4, 91–104, 1966.
- Kettle, A. J., A model of the temporal and spatial distribution of carbon monoxide in the mixed layer, M.Sc. thesis, 146 pp., Woods Hole Oceanogr. Inst.-Mass. Inst. of Technol. Joint Program in Oceanogr., Woods Hole, Mass., 1994.
- Khalil, M. A. K., and R. A. Rasmussen, The global cycle of carbon-monoxide: Trends and mass balance, *Chemosphere*, 20(1–2), 227–242, 1990.
- Kieber, D. J., J. A. McDaniel, and K. Mopper, Photochemical sources of biological substrates in seawater: Implications for carbon cycling, *Nature*, 341, 637–639, 1989.
- Leifer, A., *The Kinetics of Environmental Aquatic Photochemistry*, Am. Chem. Soc., Washington, D. C., 1988.
- Miller, W. L., and M. A. Moran, Interaction of photochemical and microbial processes in the degradation of refractory dissolved organic matter from a coastal marine environment, *Limnol. Oceanogr.*, 42, 1317–1324, 1997.
- Miller, W. L., and R. G. Zepp, Photochemical production of dissolved inorganic carbon from terrestrial organic-matter: Significance to the oceanic organic-carbon cycle, *Geophys. Res. Lett.*, 22(4), 417–420, 1995.
- Mopper, K., and D. J. Kieber, Marine photochemistry and its impact on carbon cycling, in *The Effects of UV Radiation in the Marine Environment*, Cambridge Environ. Chem. Ser., vol. 10, edited by S. de Mora, S. Demers, and M. Vernet, pp. 101–129, Cambridge Univ. Press, New York, 2000.
- Mopper, K., X. L. Zhou, R. J. Kieber, D. J. Kieber, R. J. Sikorski, and R. D. Jones, Photochemical degradation of dissolved organic-carbon and its impact on the oceanic carbon-cycle, *Nature*, 353(6339), 60–62, 1991.
- Moran, M. A., and R. G. Zepp, Role of photoreactions in the formation of biologically labile compounds from dissolved organic matter, *Limnol. Oceanogr.*, 42, 1307, 1997.
- Najjar, R. G., D. J. Erickson III, and S. Madronich, Modeling the air-sea fluxes of gases formed from the decomposition of dissolved organic matter: Carbonyl sulfide and carbon monoxide, in *The Role of Nonliving Organic Matter in the Earth's Carbon Cycle: Report of the Dahlem Workshop on the Role of Nonliving Organic Matter in the Earth's Carbon Cycle, Berlin 1993, September 12–17*, edited by R. G. Zepp and C. Sonntag, pp. 107–132, John Wiley, New York, 1995.
- Najjar, R. G., J. Werner, O. C. Zafriou, H. Xie, W. Wang, and C. D. Taylor, A one-dimensional model of carbon monoxide in Sargasso Sea surface waters, (Talk OS21K-05), *Eos Trans. AGU*, 80(49), 93, 2000.
- Nelson, N. B., D. A. Siegel, and A. F. Michaels, Seasonal dynamics of colored dissolved material in the Sargasso Sea, *Deep Sea Res.*, Part I, 45(6), 931–957, 1998.
- Ohta, K., Y. Inomata, A. Sano, and K. Sugimura, Photochemical degradation of dissolved organic carbon to carbon monoxide in coastal seawater, in *Dynamics and Characterization of Marine Organic Matter*, edited by N. Handa, E. Tanoue, and T. Hama, Terrapub/Kluwer Acad., Norwell, Mass., 1999.
- Opsahl, S., and R. Benner, Distribution and cycling of terrigenous dissolved organic matter in the ocean, *Nature*, 386(6624), 480–482, 1997.
- Opsahl, S., and R. Benner, Photochemical reactivity of dissolved lignin in river and ocean waters, *Limnol. Oceanogr.*, 43, 1297–1304, 1998.
- Redden, G. D., Characteristics of photochemical production of carbon monoxide in seawater, M. Sc. thesis, Oregon State Univ., Corvallis, Ore., 1982.
- Sarmiento, J. L., and E. T. Sundquist, Revised budget for the oceanic uptake of anthropogenic carbon-dioxide, *Nature*, 356(6370), 589–593, 1992.
- Siegel, D. A., Global distribution and dynamics of chromophoric dissolved organic matter: Implications for marine photochemistry, paper presented at Aquatic Sciences Meeting, Am. Soc. of Limnol. and Oceanogr., Waco, Tex., 2001.
- Siegel, D. A., and A. F. Michaels, Quantification of non-algal light attenuation in the Sargasso Sea: Implications for biogeochemistry and remote sensing, *Deep Sea Res.*, Part II, 43(2–3), 321–345, 1996.
- Sommaruga, R., I. Obermosterer, G. J. Herndl, and R. Psenner, Inhibitory effect of solar radiation on thymidine and leucine incorporation by freshwater and marine bacterioplankton, *Appl. Environ. Microbiol.*, 63, 4178–4184, 1997.
- Springer-Young, M., D. J. Erickson, and T. P. Carsey, Carbon monoxide gradients in the marine boundary layer of the North Atlantic Ocean, *J. Geophys. Res.*, 101(D2), 4479–4484, 1996.
- Swinnerton, J. W., V. J. Linnenbo, and R. A. Lamontag, Ocean: A natural source of carbon monoxide, *Science*, 167(3920), 984–986, 1970.
- Tolli, J., C. D. Taylor, and O. C. Zafriou, Surface light inhibition of biological CO oxidation in the Sargasso Sea: Results of an in situ ¹⁴C-CO incubation technique, paper presented at ASLO Meeting, Am. Soc. of Limnol. and Oceanogr., Copenhagen, Denmark, June 5–9, 2000.
- Valentine, R. L., and R. G. Zepp, Formation of carbon-monoxide from the photodegradation of terrestrial dissolved organic-carbon in natural-waters, *Environ. Sci. Technol.*, 27(2), 409–412, 1993.
- Vodacek, A., et al., Seasonal variation of CDOM and DOC in the Middle Atlantic Bight: Terrestrial inputs and photooxidation, *Limnol. Oceanogr.*, 42, 674–686, 1997.
- Walsh, J. J., *On the Nature of Continental Shelves*, Academic, San Diego, Calif., 1998.
- Weiss, P., S. S. Andrews, J. E. Johnson, and O. C. Zafriou, Photoproduction of COS in South Pacific Waters as a function of irradiation wavelength, *Geophys. Res. Lett.*, 22, 215–218, 1995.
- Xie, H., O. C. Zafriou, W. Wang, and C. D. Taylor, A simple automated continuous flow equilibration method for measuring carbon monoxide in seawater, *Environ. Sci. Technol.*, 35(7), 1475–1480, 2001.
- Xie, H., S. S. Andrews, W. R. Martin, J. Miller, L. Ziolkowski, C. D. Taylor, and O. C. Zafriou, Validated methods for sampling and head-space analysis of carbon monoxide in seawater, *Mar. Chem.*, 77(2–3), 93–108, 2002.
- Yocis, B. H., D. J. Kieber, and K. Mopper, Photochemical production of hydrogen peroxide in Antarctic waters, *Deep Sea Res.*, Part I, 4(6), 1077–1099, 2000.
- Ziolkowski, L. A., Marine photochemical production of carbon monoxide, M.Sc. thesis, 121 pp., Dalhousie Univ., Halifax, N. S., Canada, 2000.
- Zuo, Y., and R. D. Jones, Formation of carbon-monoxide by photolysis of dissolved marine organic material and its significance in the carbon cycling of the oceans, *Naturwissenschaften*, 82(10), 472–474, 1995.

S. S. Andrews, Department of Zoology, University of Cambridge, Cambridge CB2 3EJ, UK. (Ssa28@hermes.cam.ac.uk)

W. Wang and O. C. Zafriou, Woods Hole Oceanographic Institution, Woods Hole, MA 02543, USA. (wwang@whoi.edu; ozafriou@whoi.edu)

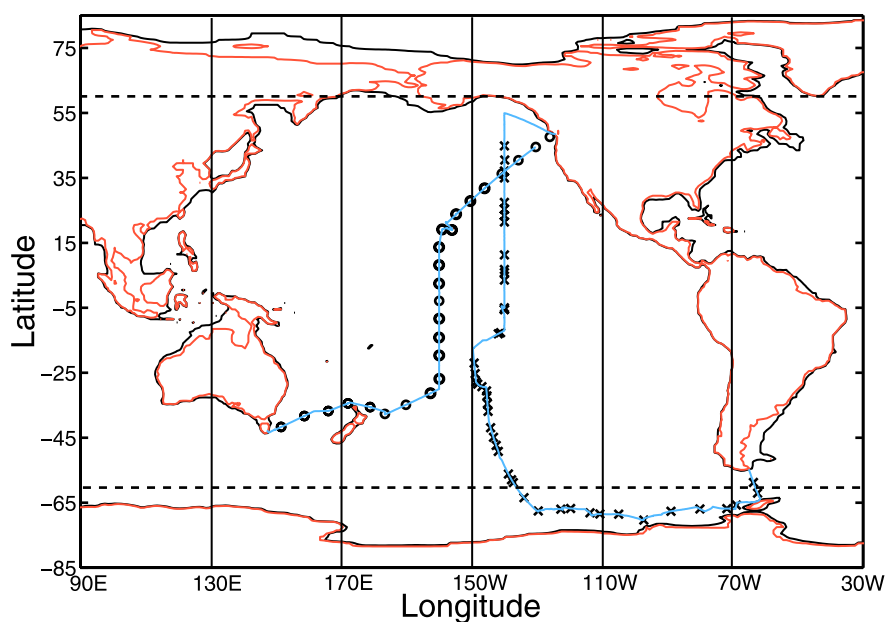


Figure 1. Cruise tracks and sample locations for ACE-1 (circles) (Southern Hemisphere Marine Aerosol Characterization Experiment, R/V *Discoverer*) and RITS-94 (crosses) (Radiatively Important Trace Species, R/V *Surveyor*). See Table 2 for sampling locations. Black contour lines offshore indicate the 200-m isobath. Areas <200 m or greater than 60° north and south (marked with dashed horizontal lines) are excluded from our global “blue-water” estimation.